Plasma Sources Science and Technology

Electrical characteristics and electron heating mechanism of an inductively coupled argon discharge

To cite this article: V A Godyak *et al* 1994 *Plasma Sources Sci. Technol.* **3** 169

Plasma Sources Sci. Technol. 3 (1994) 169–176. Printed in the UK

Electrical characteristics and electron heating mechanism of an inductively coupled argon discharge

V A Godyak, R B Piejak and B M Alexandrovich
Osram Sylvania Inc., 100 Endicott Street, Danvers, MA 01923, USA

Received 6 August 1993, in final form 8 October 1993

Abstract. The external electrical characteristics of inductively coupled argon RF discharges at 13.56 MHz have been measured over a wide range of power at gas pressures ranging from 3 mTorr to 3 Torr. External parameters, such as coil voltage, current and phase shift, were measured. From these measurements the equivalent discharge resistance and reactance, the power transfer efficiency and the coupling coefficient between the primary coil and the plasma were determined as a function of discharge power and gas pressure. The efficient RF power transfer and the large value of the effective electron collision frequency found here at low gas pressure suggest some collisionless electron heating mechanisms. This mechanism is identified as non-local electron heating in the inhomogeneous RF field due to spatial dispersion of the plasma conductivity.

1. Introduction

Low-pressure inductively coupled RF discharge sources have important industrial applications mainly because they can provide a high-density electrodeless plasma source with low ion energy and low power loss in the sheaths. These attractive features of inductively coupled discharges are recognized by both the plasma processing and the lighting community and therefore the study of these types of discharges has been actively pursued, especially over recent years.

Although inductive discharges are being vigorously studied [1–4], few data can be found in the literature about the external electrical characteristics of the induction coil that drives the discharge. This is not to say that voltage and current measurements of the induction coil for a specific point cannot be found in the literature but that a comprehensive set of measurements over a wide range of inductive discharges operation is indeed unavailable. A comprehensive set of measurements could provide a basis for the development of scaling laws for the external and internal discharge characteristics from which control of RF discharges and optimization of plasma processes could be achieved. The measurement of discharge and plasma parameters over a wide range of external conditions given here is valuable for inductive RF discharge modelling and possibly as a database for comparison of theory with experiment.

The objective of this work is to report on measurements of the external electrical characteristics of an inductively coupled discharge over a wide range of operating parameters. Measurements of the voltage, current and phase shift on the primary coil of an inductive discharge have been made over a range of power between about 20 W and 180 W and over a range of argon gas pressure between 3 Torr, where electron–neutral (e–n) collisions dominate, and 3 mTorr where e–n collisons are considerably reduced. From these measurements, the resistive (ohmic) and reactive components of the primary coil impedance, the power transfer efficiency, the minimal maintenance power and the effective electron collision frequency have been determined based on an approach developed by Piejak *et al* [4]. At low gas pressure, the effective electron collision frequency has been shown to exceed the electron–atom collision frequency considerably, suggesting that a collisionless dissipative process is responsible for electron heating. This heating is shown to be the result of spatial dispersion of the plasma conductivity in an inhomogeneous RF field, a phenomenon underlying the anomalous skin effect. The estimation of the effective electron collision frequency based on this concept is in reasonable agreement with experiment.

2. Experimental set-up

Measurements were made in a discharge chamber formed by a glass cylinder with an ID of 14.3 cm and an OD of 15.0 cm and limited at each end of the cylinder by aluminium plates 6.7 cm apart. A sketch of the discharge vessel and location of the discharge induction (primary) coil is shown in figure 1(*a*). All measurements were made with argon gas flow to enhance gas purity. The discharge chamber and vacuum–gas flow system have been described elsewhere [5]. This set-up varies from previ-

0963-0252/94/020169 + 08 $19.50

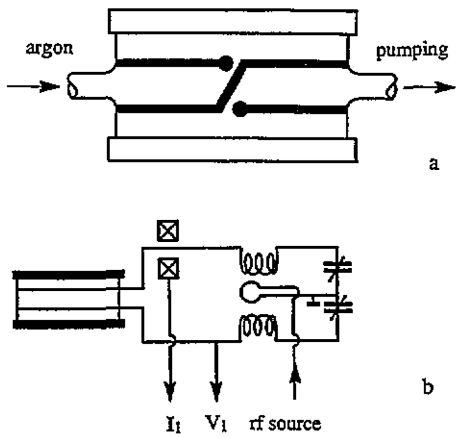

Figure 1. (a) A diagram of the experimental test chamber consisting of a glass cylinder about which a two-turn coil is wound bounded by aluminium upper and lower plates. (b) A simplified schematic diagram of the symmetrical matching system attached to an induction coil. Measurement points for discharge voltage, current and transmitted power are indicated.

ous work [4] in that the induction coil is attached to the exterior of the glass cylinder. The induction coil consists of two turns of 0.3 cm wide copper foil strip separated by 2.0 cm and is connected as shown in figure 1. With the coil and aluminium plates positioned as shown and no plasma present, the effective inductance L_0 and resistance R_0 of the unloaded coil (including leads to the matching system) were measured at 13.56 MHz and found to be 0.84 μH and 0.65 Ω respectively. In this paper the inductor with plasma present (loaded) will be referred to as the primary coil, otherwise (with no plasma) it will be referred to as the unloaded coil. Note that the aluminium plates reduce the initial coil inductance by about 15% suggesting that the RF field is localized about the coil winding and loosely coupled to the plates.

A simplified schematic diagram of the matcher circuit showing the electrical measurement points is given in figure 1(b). The source of discharge power is an RF amplifier that delivers power to a link coupled matching system. The secondary coils of the matcher are arranged so as to form a symmetric (push–pull with respect to ground) source of RF power for the induction coil and discharge. For a given discharge current, a symmetric source reduces the capacitive coupling which may affect the electrical characteristics of the discharge, especially at low RF power. The RF voltage is measured with a voltage divider directly at the input of the induction coil and current is measured with a current transformer as shown in figure 1(b). These measurements are made with a vector voltmeter in which the phase shift between the current and voltage is also measured. The incident and reflected powers are also measured in the line between the RF source and the matcher. In conjunction with a calibration curve to account for matcher losses [6], these measurements serve as an independent check of the power determined from the vector voltmeter measurements. The agreement between the two measurement techniques is generally within a few per cent. Errors in voltage and current measurements in this system [5–7] are less than or equal to about 5% while error in relative phase shift is about 0.1° which corresponds to about a 10% error in the worst case of the smallest power factor ($\cos\phi = 0.02$) measured in this work.

3. Measurement results

The primary current of the induction coil against total power is shown in figure 2. Only data for two gas pressures are shown in this figure but these data are qualitatively representative of discharge behaviour at all gas pressure and power levels considered here. At a fixed gas pressure the primary current increases with power while at a given power level the primary current is smaller at the higher gas pressure. The RF voltage across the primary coil against the total power is shown in figure 3. The trends in coil voltage against power are qualitatively similar to that of the coil current. The power factor for these two gas pressures is shown in figure 4. In all cases the power factor increases more rapidly with power at lower power levels and less rapidly at higher power levels. At a given power level, the power factor increases with gas pressures.

The external electrical characteristics of an inductive discharge may be given in terms of the equivalent coil resistance and reactance against total RF power. The primary coil resistance against total power is shown in figure 5. At each gas pressure the equivalent resistance of the primary coil increases with power and reaches a plateau at the higher gas pressures. For a fixed power, the primary resistance increases with gas pressure. The increase in equivalent resistance represents coupling of the plasma resistance into the primary coil circuit and is fundamental in the power transfer from the primary coil to the secondary (plasma) of an air coil transformer. Since with increasing power the resistance of the pri-

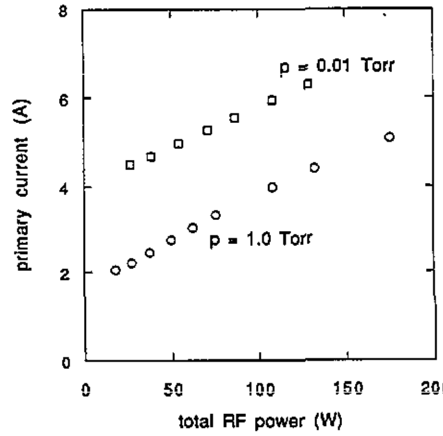

Figure 2. Current (RMS) through the primary induction coil as a function of the total RF power delivered to the coil for gas pressures of 0.01 and 1.0 Torr.

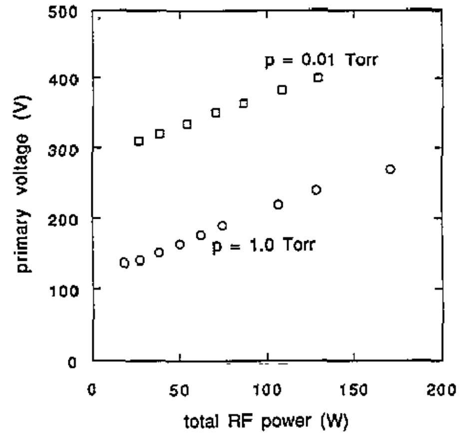

Figure 3. Voltage (RMS) across the primary coil as a function of the total RF power delivered to the coil for gas pressures of 0.01 and 1.0 Torr.

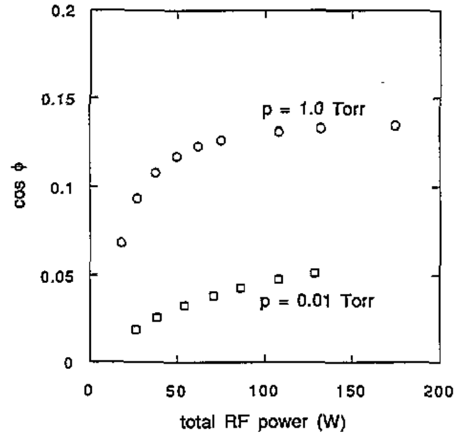

Figure 4. Power factor against total RF power over a power range between 20 and 180 W.

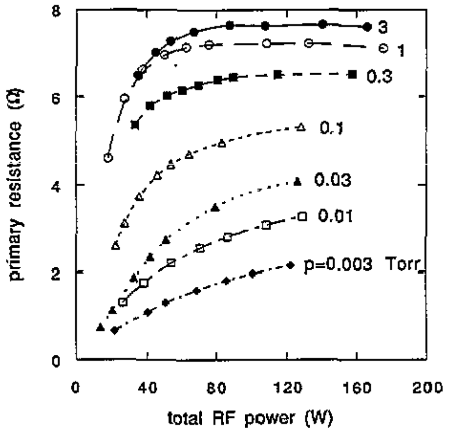

Figure 5. Primary resistance against total RF power for argon gas pressures between 3 mTorr and 3 Torr.

mary coil itself R_0 is virtually constant, the increase in primary resistance is directly related to an increase in the power transferred to the plasma.

The equivalent primary coil reactance versus power is given in figure 6. At a fixed gas pressure the primary reactance decreases with total power while at a fixed power level the primary reactance decreases with increasing gas pressure. As in the case of equivalent resistance the reduction in primary reactance reflects an

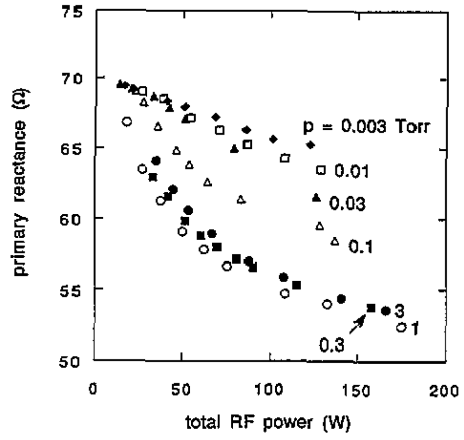

Figure 6. Primary coil reactance against total RF power for argon gas pressures between 3 mTorr and 3 Torr.

increase in the mutual coupling between the coil and the plasma. Essentially, the plasma current flow partially *neutralizes the time varying magnetic flux created by* current flow through the primary coil. Thus, a reduction in the primary equivalent reactance represents the diamagnetic effect of the plasma coupled to the primary coil.

4. Evaluation of internal discharge parameters

From direct measurements of the external electrical characteristics of the discharge, spatially integrated internal discharge parameters can be inferred [4]. These parameters are the power dissipated in the plasma P_2, the minimal inductive discharge power P_0, the coupling coefficient k between the primary coil and the plasma and the Q factor of the secondary (plasma) circuit Q_2 (which is the ratio between the reactance and the resistance of the secondary circuit including the plasma). Some of these parameters are unique functions of external (given) discharge parameters: geometry, frequency, gas type and pressure and total RF power while others may be expressed as an average over a certain RF power range or over the range of another external parameter. The basis for inferring these internal parameters is the transformer theory equations (see, for example the work of Piejak *et al* [4]) which in essence are spatial integrals *of Maxwell's equations:*

$$\rho = R_1 - R_0 = \omega^2 k^2 L_0 L_2 R_2 / Z_2^2 \qquad (1)$$

$$\zeta = \omega(L_0 - L_1) = \omega^2 k^2 L_0 L_2 (\omega L_2 + \omega/\nu_{\mathrm{eff}} R_2)/Z_2^2 \qquad (2)$$

where ρ and ζ correspond to changes in primary resistance and reactance (for a series equivalent circuit) due to plasma loading; R_0 and $\omega L_0 = X_0$ correspond to the unloaded coil resistance and reactance; R_1 and ωL_1 correspond to the primary resistance and reactance with plasma; L_2 and R_2 are the magnetic inductance and *ohmic resistance (plasma resistance) of the secondary* circuit; $Z_2 = [(\omega L_2 + \omega/\nu_{\mathrm{eff}} R_2)^2 + (R_2)^2]^{1/2}$ is the impedance of the secondary circuit; and ν_{eff} is the effective electron collision frequency accounting for RF power dissipation process in the inductive RF plasma [4].

Expressions for k, Q_2 and P_2 directly follow from equations (1) and (2):

$$k^2 = (\zeta^2 + \rho^2)/X_0(\zeta - \rho\omega/\nu_{eff}) \tag{3}$$

$$Q_2 \equiv \omega L_2/R_2 + \omega/\nu_{eff} = \zeta/\rho \tag{4}$$

$$P_2 = I^2\rho. \tag{5}$$

From the measured external electrical parameters these parameters can be found for each point of discharge operation. Moreover, they can be found for any arbitrary inductive RF discharge, without prior knowledge of a particular discharge geometry or spatial distribution of plasma and the electromagnetic field.

In our experimental arrangement the aluminium end plates affect the unloaded coil inductance to an extent comparable to that caused by the plasma. However, since the plate conductivity and position referenced to the unloaded coil remains unchanged throughout the experiment, the influence of the plates is accounted for in the unloaded coil characteristic constants X_0 and R_0 (measured with the plates and no plasma). Only in a strong skin effect regime, when RF field distribution is significantly affected by the plasma, might one expect some change in X_0 and R_0, however, as will be shown, this case is not encountered in these experiments.

Having inferred RF power absorbed by the plasma P_2, power transfer efficiency η is simply P_2/P_1. Figure 7 represents η as a function of the total RF power P_1 for argon pressure between 3 mTorr and 3 Torr. In general, $\eta(P_1)$ drops at small and decreasing P_1 as P_1 approaches the minimal maintenance power P_0 (dissipated in the unloaded coil, $P_0 = I_1^2 R_0$ as $P_2 \to 0$) needed to induce an RF electric field sufficient to maintain the plasma. As shown by Piejak *et al*

$$P_0 = (1 + \omega^2/\nu_{eff}^2)V_2^2/k^2 Q_0 \omega L_2 \tag{6}$$

where $V_2 = (P_2 R_2)^{1/2}$ is the ohmic component of the secondary voltage and Q_0 is the Q factor of the unloaded primary coil. P_0 varies with gas pressure, since the ohmic component of plasma voltage V_2 (governed by ionization and energy balance) as well as the factor ω/ν_{eff} depend on the gas pressure. The minimal maintenance power P_0 is the power in the primary coil in the limit $P_2 \to 0$ and can be found from the measurements of the primary current I_1 as $P_0 = I_{10}^2 R_0$, where $I_{10} = I_1$ as $P_2 \to 0$.

In figure 8 the primary current I_1 is shown as a function of the discharge power P_2 for different argon pressures. Extrapolating $I_1(P_2)$ to the limit $P_2 = 0$ gives an estimate of I_{10} and P_0. From figure 8 for $p = 1.0$, 0.1, 0.01 and 0.003 Torr the corresponding values of I_{10} are 1.7, 2.5, 4.2, and 5.7 A, resulting in a minimal maintenance power P_0 of 1.9, 4.0, 11.5, and 21 W respectively. Thus, as shown in [4], power loss in the primary coil generally increases with decreasing gas pressure thereby reducing power transfer efficiency to the plasma load. As one can see in figure 7 the power transfer efficiency grows with RF power, and according to [4] reaches a broad maximum at the condition when the secondary magnetic reactance equals the plasma impedance:

$$\omega L_2 = R_2(1 + \omega^2/\nu_{eff}^2)^{1/2}. \tag{7}$$

It seems (from figure 7) that such a condition is reached for relatively large argon pressure ($p = 0.3$–3 Torr) where collisionally dominated electron heating processes occur through electron–atom collisions ($\nu_{eff} = \nu_{en}$) and $\omega^2/\nu_{en}^2 \ll 1$, where ν_{en} is the electron–atom collision frequency. At these pressures RF power is efficiently transferred to the plasma over a wide range of total RF power and $\eta \approx 0.9$. At lower argon pressure ($p = 3$–30 mTorr) η is somewhat smaller ($\eta = 0.4$–0.8) but does not drop as dramatically as expected [4] for collisional heating and $\omega^2/\nu_{en}^2 \gg 1$.

Preliminary probe measurements of the electron energy distribution function in this discharge at $p = 10$ mTorr allowed us to estimate (using the electron–atom cross section for argon) the electron–atom collision frequency $\nu_{en} \approx 2.0 \times 10^6$ s^{-1} suggesting that $\omega/\nu_{en} \approx$

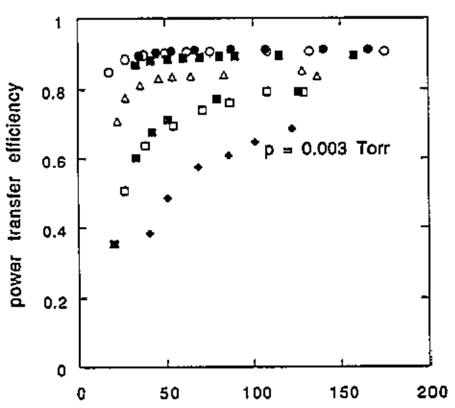

Figure 7. Power transfer efficiency against total RF power for argon gas pressures between 3 mTorr and 3 Torr. The symbols for pressure are the same as in the previous figures.

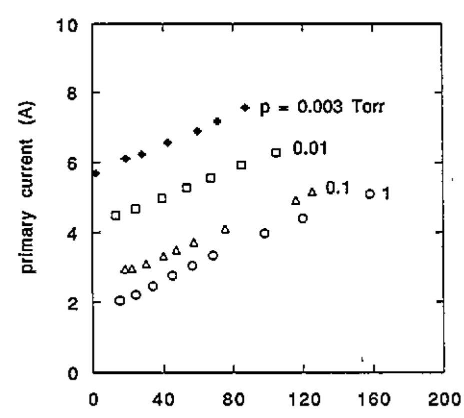

Figure 8. The primary RF current against discharge power for $p = 0.003$, 0.01, 0.1 and 1 Torr.

40. For this value of ω/ν_{en} one can then obtain [4] the power transfer efficiency:

$$\eta \leqslant (1 + 4k^{-2}Q_0^{-1}\omega/\nu_{en})^{-1} = 0.25 \qquad (8)$$

where the sign of equality on the left-hand side of expression (8) corresponds to the matching condition (7).

Assuming a collisional electron heating process at $p = 10$ mTorr, η should be no more than 0.25, whereas experimental data plotted in figure 7 show much larger values of η (up to $\eta = 0.8$). An even larger difference between collisional and experimental values of η is expected for $p = 3$ mTorr. Thus, at low pressure there is some additional non-collisional dissipation process, such that $\nu_{eff} > \nu_{en}$.

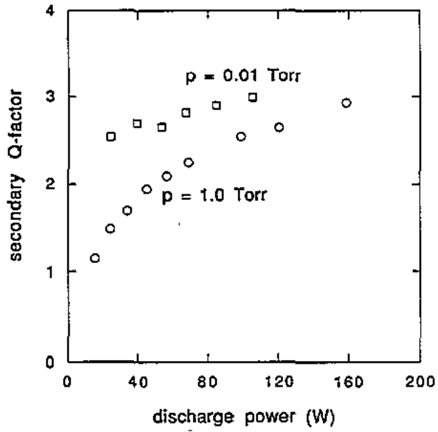

Figure 9. The Q factor of the secondary circuit against the discharge power for 0.01 and 1 Torr.

5. Effective electron collision frequency

It appears to be possible to infer the value of ν_{eff} from measured electrical characteristics of the primary coil using equation (4), although the parameter $\omega L_2/R_2$ in this equation remains unknown. This can be done in a number of ways. First, the ratio ω/ν_{eff} can be found at the specific value of P_1 corresponding to the matching condition (7) when the power transfer efficiency $\eta(P_1)$ is maximal:

$$\omega/\nu_{eff} = 1/2(\zeta/\rho - \rho/\zeta). \qquad (9)$$

Unfortunately, at low pressure, the matching condition does not appear to be reached within the RF power interval of the present experiment. Another way to find ν_{eff} is at the condition when $\omega L_2/R_2 \ll \omega/\nu_{eff}$ which occurs in the limit of small discharge power P_2. Noting that $R_2 = V_2^2 P_2^{-1}$, equation (4) may be rewritten in the following form:

$$\zeta/\rho = \omega L_2 P_2/V_2^2 + \omega/\nu_{eff} = Q_2 \qquad (10)$$

from where in the limit as $P_2 \to 0$ one obtains:

$$\omega/\nu_{eff} = \zeta/\rho. \qquad (11)$$

Experimental values of $Q_2 = \zeta/\rho$ are given in figure 9 as functions of the discharge power P_2 for $p = 10$ mTorr and 1.0 Torr. Extrapolation of the experimental data of ζ/ρ for $p = 10$ mTorr to the point where $P_2 = 0$ yields a value of $\omega/\nu_{eff} = 2.2$ corresponding to $\nu_{eff} = 3.9 \times 10^7$ s^{-1} which is more than an order of magnitude larger than the electron–atom collision frequency ν_{en}. The corresponding calculation for $p = 3$ mTorr gives $\nu_{eff} \approx 2.0 \times 10^7$ s^{-1} which also greatly exceeds ν_{en} at this pressure. As seen in figure 9, at $p = 10$ mTorr, ζ/ρ grows linearly with P_2 inferring, according to equation (10), that the ratio $\omega L_2/V_2^2$ is nearly constant. This seems reasonable since both L_2 which is governed by the RF field and plasma distributions and V_2 which is proportional to the plasma RF field, are nearly independent of P_2 at low gas pressures.

A different behaviour for ζ/ρ with P_2 is seen for $p = 1.0$ Torr. Although as expected for $\omega/\nu_{en} \ll 1$, $\zeta/\rho \to 0$ as $P_2 \to 0$, the value of $\omega L_2/V_2^2$ does not stay constant when P_2 grows. This is probably the result of discharge constriction due to gas heating at higher pressure and may also be due to the skin effect, both being more pronounced at higher discharge power. Both effects decrease the discharge channel cross section and move it closer to the primary coil winding, finally resulting in a rising coupling coefficient and discharge voltage V_2. Visual contraction with growing RF power could be seen in our experiments at higher argon pressure. This phenomena of discharge constriction is well known in DC discharges at high current and gas pressure.

A third way of finding ω/ν_{eff} comes directly from equation (3).

$$\omega/\nu_{eff} = \xi/\rho - (\xi + \rho^2)/k^2 X_0 \rho. \qquad (12)$$

Here the coupling coefficient k remains unknown, but since $k < 1$, one can evaluate the lowest possible value of $\nu_{eff\text{-}min}$ (at $k = 1$) suggesting:

$$\nu_{eff} > \nu_{eff\text{-}min} = \omega[\xi/\rho - (\xi^2 + \rho^2)/X_0\rho]^{-1}. \qquad (13)$$

The calculation of $\nu_{eff\text{-}min}$ for $p = 10$ mTorr over the entire interval of discharge power (20 W $\leqslant P_2 \leqslant$ 100 W) gives $\nu_{eff\text{-}min}$ between 3.47×10^7 s^{-1} and 3.27×10^7 s^{-1} both of which are just slightly less than $\nu_{eff} = 3.9 \times 10^7$ s^{-1} found from using equations (10) and (11).

The influence of the coupling coefficient k on the inferred value of ν_{eff} is shown in figure 10 where ratios of ω/ν_{eff} calculated using equation (12) are given as function of discharge power for different values assigned to k. Two interesting features can be seen in figure 10. First, for all reasonable values of k ($0.3 \leqslant k \leqslant 1.0$), in the limit of $P_2 = 0$ the calculated values of ω/ν_{eff} converge well to the value of $\omega/\nu_{eff} = 2.2$ found earlier. Second, if one assumes that the real value of k is that one which provides constant values for the inferred value of ω/ν_{eff} the result would again be $\omega/\nu_{eff} = 2.2$ or $\nu_{eff} = 3.9 \times 10^7$ s^{-1}. Thus, the effective electron collision frequency found in different ways gives a value of $\nu_{eff} \approx 4 \times 10^7$ s$^{-1} \gg \nu_{en} \approx 2 \times 10^6$ s^{-1}. This result suggests some non-collisional dissipation process responsible for RF power

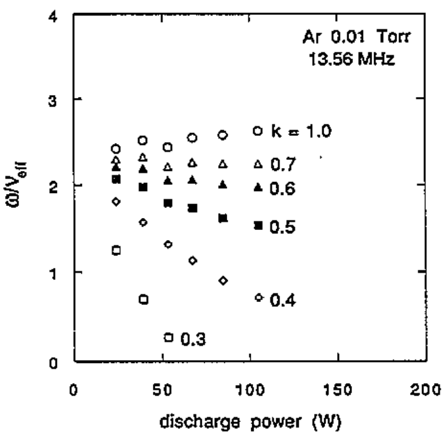

Figure 10. The inferred ratio of ω/ν_{eff} against discharge power for fixed values of k between 0.3 and 1.

transfer to the plasma electrons in the low-pressure inductive RF discharge.

Prior to discussing a possible mechanism of collisionless power transfer the coupling coefficient k should be evaluated. This readily follows from equation (3) provided that the ratio ω/ν_{eff} is known. For high argon pressure ($p > 0.3$ Torr) where $\nu_{eff} = \nu_{en}$ and $\omega/\nu_{eff} \ll \xi/\rho \approx 1 - 3$,

$$k^2 = (\xi^2 + \rho^2)/\xi X_0. \qquad (14)$$

The values of k found using equation (14) for $p = 1$ Torr are shown in figure 11. Results for $p = 10$ mTorr found using equation (3) and $\omega/\nu_{eff} = 2.2$ inferred for this pressure are also shown. Note that the values of k found for low pressures from equation (3) are very sensitive to the particular value of ω/ν_{eff}. Small deviations in ω/ν_{eff} lead to significant dispersion in the values of k. That is why at low pressures when $\omega/\nu_{eff} \geqslant 1$ it seems more reliable to find k as that which provides the minimal deviation of ω/ν_{eff} with discharge power as shown in figure 10. Since in this case k is found as some averaged value over the range of discharge power, this way of inferring k is applicable when plasma density and RF field distributions do not change appreciably with discharge power. This takes place at low gas pressure and moderate discharge power, when the skin depth is not much smaller than the plasma's characteristic dimension [2].

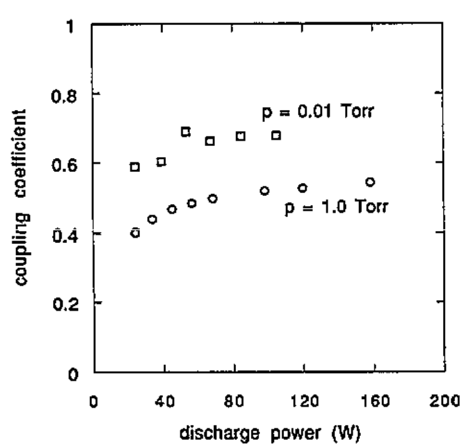

Figure 11. Coupling coefficient against power dissipated in the discharge for gas pressures of 0.01 and 1.0 Torr.

6. Collisionless RF heating in an inductively coupled discharge

Collisionless electron heating is now commonly accepted as a primary mechanism in sustaining low-pressure capacitive RF discharges. It occurs at the plasma–sheath interface as a result of inelastic electron reflection from the oscillating RF electrode sheaths. Contrary to capacitive RF discharges, the RF current in an inductively coupled discharge is closed within the plasma and does not form an oscillating RF sheath. Since some capacitive coupling between the primary coil and the inductive plasma (through the glass wall) takes place, one might suggest that capacitive coupling may be responsible for the collisionless (stochastic) electron heating in the wall sheath. However, it has been demonstrated that capacitively coupled RF discharges maintained in the same discharge chamber [7] (using parallel plates as RF electrodes having an order of magnitude larger surface area than the primary coil) dissipate an order of magnitude less power than in a inductive discharge under the same RF voltage and gas pressure. Thus, capacitive effects on the inductive discharge appear to affect the energy balance by only about 1% at low pressure. A more precise estimation of capacitive effects has been done by comparing RF power consumed in the capacitive mode with the primary coil cut in the middle with that consumed in the inductive mode with an equal RF voltage applied to the primary coil. At $p = 10$ mTorr and P_2 between 20 and 100 W this experiment showed that the influence of capacitive effects on the discharge energy balance is less than 1%. Therefore, we have to conclude that in this experiment stochastic electron heating in the wall sheath is negligible.

We believe that the collisionless RF power dissipation mechanism in low pressure inductive RF discharges (first found and reported by Godyak and Piejak [8]) is related to the phenomenon, discovered for superconductors by Pippard [9] almost a half century ago, known as the anomalous skin effect [10, 11]. This effect occurs in superconductors and collisionless plasmas when the skin depth δ is smaller than the electron mean free path for momentum transfer λ_e. Under this condition the well known formula for normal (resistive) skin depth δ_n:

$$\delta = \delta_n \equiv c(2\pi\omega\sigma)^{-1/2} \equiv c/\omega_e(2\nu_{en}/\omega)^{1/2} \qquad (15)$$

is not applicable. Here σ is the real part of the plasma conductivity, ω_e is the electron plasma frequency and c is the speed of light in vacuum. Note that equation (15) is only valid for $\nu_{en} \gg \omega$. The validity of equation (15) for normal skin effect suggests local coupling between the RF field and the RF current within the skin layer, i.e. $\lambda_e \ll \delta$. For the opposite case when $\lambda_e \gg \delta$ there no longer is local coupling between the RF field and the RF current within the skin layer. Due to thermal electron motion, electrons accelerated in the skin layer create an RF current outside of the skin layer. This effect, known as spatial dispersion of the plasma conductivity [10], leads to the expression of skin depth for the anomalous skin effect [9, 11]:

$$\delta = \delta_a \equiv c/\omega_e(4v_{Te}\omega_e/c\omega)^{1/3} \tag{16}$$

where v_{Te} is the electron thermal velocity, $v_{Te} = (8kT_e/\pi m)^{1/2}$.

Expression (16) is valid for $\omega \ll v_{Te}/\delta$, meaning that electrons cross the skin layer in less time than the RF field period [11], i.e. the electrons practically move as in a DC field, gaining energy from the RF field localized in the RF skin layer. This essentially differs from collisionless electron motion in a homogeneous RF field where electrons gain energy in one half cycle of the RF field and return the energy back in the other half of the cycle. There is no electron heating in the RF field unless some phase mixing mechanism breaks the regularity in the electron oscillation. For collisional heating this occurs due to electron–atom (and/or ion) collisions. In the case of the anomalous skin effect the mixing mechanism is provided by the electron thermal motion (spatial dispersion) which moves electrons out of the skin layer to the neighbouring plasma with no RF field, thus preventing electrons from returning the energy acquired in the skin layer back to the RF field.

The anomalous skin effect outlined here could explain the collisionless electron heating in the skin effect controlled (skinned) inductive RF discharge, which occurs when the RF field space distribution in the plasma $E(r)$ is significantly affected by the plasma conductivity and differs from that with no plasma $E_0(r)$, but we have no evidence from our experiment that this is the case. Our estimation of the skin depth for $p = 10$ mTorr and $P_2 = 50$ W using formulae (15) and (16) and that for the non-dissipative (reactive) skin depth $\delta_0 = c/\omega_e$, all give about the same value for $\delta_n \approx \delta_a \approx \delta_0 \approx 3$–$3.5$ cm. Moreover, these are very close to the characteristic length of the RF field inhomogeneity in the absence of a plasma, $\Lambda_0 = [\text{grad} \ln E_0(r)]^{-1} \approx 3$ cm. For the coil configuration in our experiment, Λ_0 is determined by the coil pitch rather than by its radius. The estimated numbers cannot support either a certain kind of skin effect or even the importance of the skin effect at all under the conditions of our experiment. However, we would like to state here that the space dispersion mechanism which governs the anomalous skin effect should work in a low-pressure inductive discharge independent of whether the discharge is in a skinned regime or not.

Indeed, the dissipative mechanism underlying the anomalous skin effect originates not by the skin effect itself (due to electromagnetic induction caused by the plasma current) but by the RF field inhomogeneity which is always the case in an inductive RF discharge. In this regard there is an essential difference between a long homogeneous conductor connected to an RF current source and a plasma maintained by an RF current flowing in the primary coil outside the plasma. In the former case the RF field inhomogeneity and accompanying collisionless dissipation arises as the result of the skin effect while in the latter case the inhomogeneous RF field and collisionless dissipation occurs whether the skin effect is present or not. In other words, in an inductively coupled plasma (independent of the plasma density) the RF field is inhomogeneous as if there is a skin effect!

Let us now evaluate the effective electron collision frequency v_{eff} corresponding to the RF energy dissipation due to spatial dispersion in the inhomogeneous RF field. As pointed out by Pippard [9] for the anomalous skin effect, the length of the electron–RF field interaction is equal to the skin depth $\delta_a \gg \lambda_e$, contrary to the normal skin effect where the interaction length is equal to the electron mean free path $\lambda_e \ll \delta_n$. Accordingly, collisionless dissipation due to spatial dispersion in general is governed by the length of the electron–RF field interaction equal to the RF field inhomogeneity length:

$$\Lambda = [\text{grad} \ln E(r)]^{-1} \tag{17}$$

which in the specific case of the skinned discharge ($\delta_a \ll \Lambda_0$) is equal to the skin depth ($\Lambda = \delta_a$). Therefore, v_{eff} in the expression for the real part of the plasma conductivity, $\sigma = \omega_e^2/4\pi v_{eff}$, used in the model [4] and in the derivation of the present work, can be evaluated as follows

$$v_{eff} = a v_{Te}/\Lambda \tag{18}$$

where a is some constant number of the order of one. This constant can be found by substituting equation (18) instead of v_{en} in equation (15) and equating it to equation (16) for the anomalous skin depth. Such a procedure yields $a = 2$ and

$$v_{eff} = 2v_{Te}/\Lambda. \tag{19}$$

For Λ_0 estimated earlier to be around 3 cm and $v_{Te} \approx 8 \times 10^7$ cm s^{-1} (calculated from probe measurements) found from equation (19) $v_{eff} \approx 5.3 \times 10^7$ s^{-1} is very close to that from our experiment, $v_{eff} \approx 3.9 \times 10^7$ s^{-1}.

7. Conclusions

Electrical characteristics of the primary coil of an inductively driven low-pressure RF discharge have been measured over a wide range of discharge conditions. These measurements show general trends and relationships (experimental scaling laws) for basic electrical parameters of inductively driven plasma as a function of RF power and gas pressure. Based on a macroscopic analysis approach previously developed [4] some discharge integral characteristics, important for practical use of inductively driven plasmas, have been inferred. Because of the complicated geometry in this experiment it is non-trivial to infer values of the RF field and plasma density as had been done in a collision dominated inductive discharge with a long cylindrical coil [4]. Nonetheless, this can be done by making some assumptions (or numerical calculations) with reference to the relationships between the coupling coefficient and coil and plasma geometry. In this work various skin depths (collisionless, normal and anomalous) have been discussed and evaluated. However, coincidence in the values of all skin depths and the closeness of v_{eff} to ω made it impossible to make firm conclusions with regard to the governing skin effect mechanism and its relative importance in our experiments at low argon gas pressure. Fortunately, according to the concept of this work, it is not a crucial factor in defining collisionless electron heating in inductively coupled plasmas.

From direct measurements of the electrical characteristics at the primary coil we have inferred an effective electron collision frequency related to the electron heating process and we have found that it is much greater than the electron–atom collision frequency at low gas pressure. This means that in low-pressure inductive RF discharges ($\omega/v_{en} \gg 1$ and $\lambda_e \geqslant \Lambda_0$) a collisionless mechanism dominates the electron heating. We identified this mechanism as the effect of plasma conductivity dispersion and based on this mechanism estimated a value of v_{eff} which is in reasonable agreement with experiment. Note that this mechanism is not identical to the anomalous skin effect and can take place even in the absence of the skin effect, i.e. for low-density plasma and low frequency where skin depth is much larger than the plasma size. Collisionless electron heating due to plasma conductivity dispersion (or spatial dispersion) is originated by the inhomogeneity of the RF field and is very general for a collisionless plasma in an inductively coupled RF discharge.

References

[1] Eckert H U 1986 *Proc. 2nd Ann. Int. Conf. on Plasma Chemistry and Technology* ed H Boenig (Lancaster, PA: Technomic)

[2] Lister G G and Cox M 1992 *Plasma Sources Sci. Technol.* **1** 67

[3] Denneman J W 1990 *J. Phys. D. Appl. Phys.* **23** 293

[4] Piejak R B, Godyak V A and Alexandrovich B M 1992 *Plasma Sources Sci. Technol.* **1** 179

[5] Godyak V A, Piejak R B and Alexandrovich B M 1990 *Rev. Sci. Instrum.* **61** 2401

[6] Godyak V A and Piejak R B 1990 *J. Vac. Sci. Technol.* A **8** (5) 3833

[7] Godyak V A, Piejak R B and Alexandrovich B M 1991 *IEEE Trans. Plasma Sci.* **19** 660

[8] Godyak V A and Piejak R B 1992 *45th Ann. Gaseous Electronics Conf. Presentation LB-11 (Boston, MA)*

[9] Pippard A B 1949 *Physica* XV **1–2** 40, 46

[10] Lifshitz E M and Pitaevskii L P 1981 *Physical Kinetics, Landau and Lifshitz Course of Theoretical Physics* vol 10 (New York: Pergamon) p 368

[11] Alexandrov A F, Bogdankevich L S and Rukhadze A A 1984 *Principles of Plasma Electrodynamics* (Berlin: Springer) p 89